RAPID COMMUNICATIONS

PHYSICAL REVIEW B VOLUME 45, NUMBER 7 15 FEBRUARY 1992-I

Optical properties of titanium dioxide in the rutile structure

Keith M. Glassford and James R. Chelikowsky
Department of Chemical Engineering and Materials Science, Minnesota Supercomputer Institute, University of Minnesota, Minneapolis, Minnesota 55455

(Received 9 September 1991; revised manuscript received 12 December 1991)

We present first-principles calculations for the optical properties of titanium dioxide in the rutile structure. The electronic band structure has been calculated self-consistently within the local-density approximation using *ab initio* pseudopotentials and a plane-wave basis. Optical properties are determined from the imaginary part of the dielectric function and compared to experiment. Although our local-density calculation underestimates the band gap, our results show that the optical properties for this early-transition-metal oxide are in surprisingly good agreement with experiment away from the fundamental absorption edge. We attribute this good agreement to the ability of the local-density approximation to yield accurate matrix elements between occupied and empty states.

The importance of the optical and electronic properties of TiO_2 may be illustrated by its role as a dielectric material for integrated electronics, as an antireflection coating for solar cells, as a substrate in catalytic and in electrochemical processes, and as a pigment for paints and polymers. Interest in the optical properties of TiO_2 have prompted reflectance,[1] electroreflectance,[2,3] electroabsorption,[4] absorption,[5] and wavelength-modulated transmission[6] spectroscopic measurements. The interpretation and assignment of the rich optical spectrum of titania to specific electronic excitations within the Brillouin zone (BZ) depends upon accurate electronic structure calculations.

The response function for the optical properties of a solid, describing the absorption or emission of electrons or photons, is the dielectric function. One may calculate the dielectric function from accurate band-structure calculations, thereby allowing one to assign the spectral features to specific excitations within the BZ, as well as obtaining interband topologies. A successful application of this approach to the optical properties of diamond and zinc-blende semiconductors is the empirical pseudopotential method[7] (EPM). In this method, one solves Schrödinger's wave equation using a pseudopotential which is adjusted to obtain agreement with the experimental response function. An alternative method is to proceed with *ab initio or* "first-principles" methods.

Perhaps the most successful of these first-principles approaches is the local-density approximation[8] (LDA). This approach has experienced a considerable amount of success at predicting ground-state structural and cohesive properties of condensed matter systems.[9] Excited-state properties, such as the dielectric function, become questionable with the LDA. However, the resulting eigenvalues and eigenvectors are often associated with single-particle excitation energies and wave functions. For semiconductors and insulators, this association is known to lead to band gaps which are often 30% to 50% lower than experiment.[10,11] Formalisms which account for many-body effects such as the quasiparticle[10] and self-interaction correction approach[12,13] have met with some success at describing excited-state properties for simple semiconductors and insulators, and give band gaps which agree to within 0.1 eV of experiment. For simple insulators and semiconductors, these calculations result in wave functions which are virtually identical to those obtained with LDA.[10] However, these methods are computationally intensive. As shown in the present investigation, LDA can give good results for the optical properties of early transition-metal oxides. In general, transition-metal oxides are known to be very difficult to model using the LDA as is exemplified by a late-transition-metal oxide such as NiO which LDA predicts to be a metal rather than an insulator.[12] It is an open question whether reasonable results may be obtained for the optical properties of an early-transition-metal oxide such as TiO_2, which we examine in the present study.

The calculational procedure for determining the ground-state structural, electronic, and cohesive properties has been described in previous work.[14,15] Wave functions were expanded in a plane-wave basis up to a kinetic energy of 64 Ry. Integrations were performed with one special k point while the exchange-correlation potential of Ceperley and Adler[16] was used. Our norm-conserving pseudopotentials were obtained by the method of Troullier and Martins[17] and separated using a Kleinman and Bylander[18] transformation. The structural parameters used in the present calculations were previously obtained by self-consistently minimizing the total energy of the rutile structure.[14]

The optical properties have been obtained through the frequency-dependent dielectric function, $\epsilon(\omega)=\epsilon_1(\omega)+i\epsilon_2(\omega)$, using the formalism of Ehrenreich and Cohen.[19] The imaginary part of the dielectric function is given as

$$\epsilon_2(\omega)=\frac{4\pi^2e^2\hbar}{m^2\omega^2}\sum_{v,c}\frac{2}{(2\pi)^3}\int_{\mathrm{BZ}}\delta[\omega_{cv}(\mathbf{k})-\omega]\,|M_{cv}(\mathbf{k})|^2d^3k \tag{1}$$

where the integral is over the first Brillouin zone, $M_{cv}(\mathbf{k})=\langle u_{c\mathbf{k}}|\hat{e}\cdot\nabla|u_{v\mathbf{k}}\rangle$ are the dipole matrix elements for the direct transitions between valence- and conduction-band states, $\hbar\omega_{cv}(\mathbf{k})=E_{c\mathbf{k}}-E_{v\mathbf{k}}$ is the excitation energy, $\hat{e}$ is the polarization vector of the electric field, and $u_{c\mathbf{k}}(\mathbf{r})$ is the periodic part of the Bloch wave function for a conduction-band state with wave vector $\mathbf{k}$. We have self-consistently determined the eigenvalues and wave functions at 126 **k** points within the irreducible part of the BZ. Excitation energies between the valence-band and conduction-band states up to approximately 16 eV from the valence-band edge were considered. Brillouin-zone integrations have been performed within the linear analytic tetrahedron scheme[20] with an energy spacing of 0.05 eV.

Owing to the large anisotropic nature of tetragonal cell of rutile, the optical properties are strongly dependent on the direction of the incoming polarized light. When the polarization direction is perpendicular ($\mathbf{E}_\perp$) or parallel ($\mathbf{E}_\parallel$) to the c axis, a high degree of fine structure exists in the optical properties (as indicated in Table I).[1] Relating these structural features to critical points and interband topology within the BZ via Eq. (1) depends upon accurate band-structure calculations.

In Fig. 1, we show the band structure[14] for TiO_2. The tightly bound O $2s$ bands, shown in the lower panel, result in a bandwidth of 1.8 eV. The upper valence bands with a width of 5.7 eV, are composed mainly of O $2p$ states and is in good agreement with experimental values in the range of 5–6 eV.[21] A recent linear muffin-tin orbital calculation has yielded similar valence-band widths.[22] A 2.0-eV direct-forbidden gap occurs at Γ and is ~30% lower than the experimental value of 3.0 eV.[5] The lower conduction-band states, with a full width of 5.6 eV, are composed primarily of Ti $3d$ states. The lowest six bands may be associated with the t_{2g} "crystal-field" symmetry and the next four with the e_g symmetry of an octahedrally coordinated Ti atom.

The imaginary part of the dielectric function for both $\mathbf{E}_\perp$ and $\mathbf{E}_\parallel$ polarizations is shown in Fig. 2. The theoretical curves have been convoluted with a Gaussian with a half width at half maximum of 0.15 eV. The experimental values of ϵ_2 for both $\mathbf{E}_\perp$ and $\mathbf{E}_\parallel$ have been measured by Cardona and Harbeke[1] from reflectance measurements and by Vos and Krusemeyer[3] using electroreflectance spectroscopy. While both experiments yield peak positions in reasonable agreement, their amplitudes are at variance. We have chosen to compare our theoretical result to the experimental work of Cardona and Harbeke,[1] shown in Fig. 2, which are in better agreement with other experimental observations.[23] LDA underestimates the excitation energies as is evident by the shift in the fundamental absorption edge to lower energies. Beyond the absorption edge, good agreement is obtained with the experimental fine structure indicating that a single-particle

TABLE I. Comparison of the experimental critical point energies (eV) of Cardona and Harbeke (Ref. 1) to the present first-principles results for polarizations perpendicular ($\mathbf{E}_\perp$) and parallel ($\mathbf{E}_\parallel$) to the c axis. The notation of the optical peaks corresponds to Cardona and Harbeke (Ref. 1).

$\mathbf{E}_\perp$	Experiment	Theory	$\mathbf{E}_\parallel$	Experiment	Theory
A_1	4.00	3.06	A	4.11	3.06
A_2	5.35	4.67			
B_1	6.10	6.06	B	6.63	6.15
B_2	7.40	6.96			
C	8.05	7.59	C	7.87	7.27

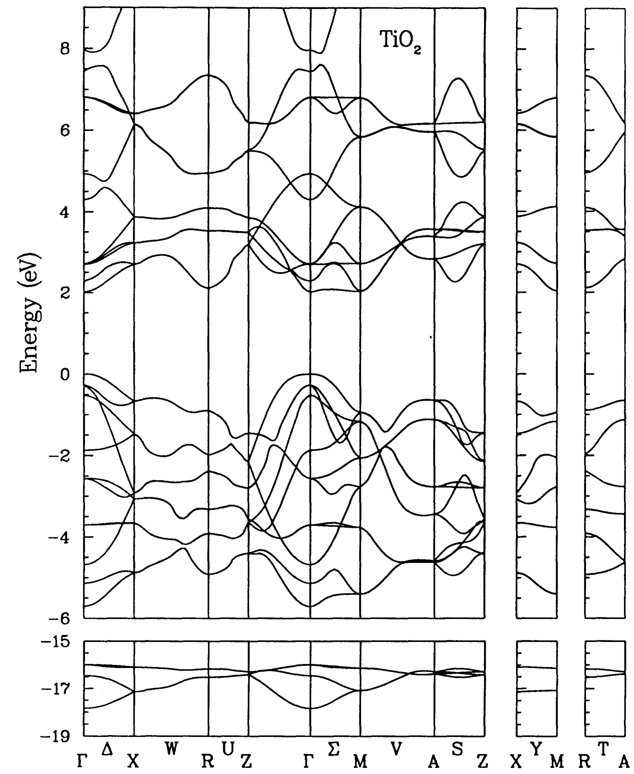

FIG. 1. Band structure for TiO_2 along the high-symmetry directions of the irreducible Brillioun zone. The valence-band maximum is taken as the zero of energy.

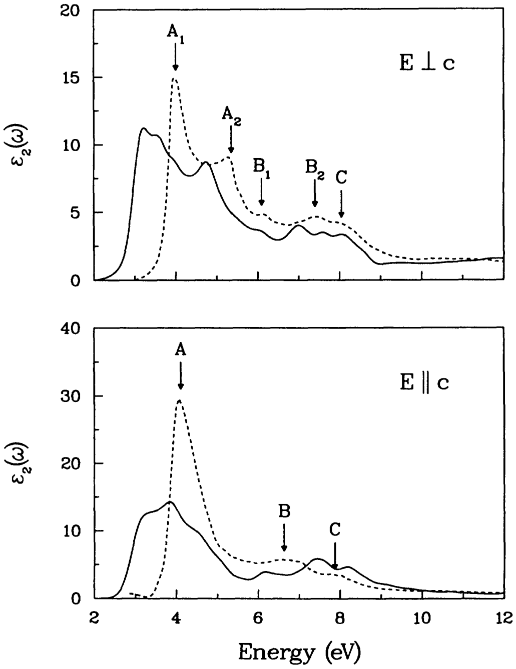

FIG. 2. The imaginary part of the dielectric function for polarization vectors perpendicular $\mathbf{E}_\perp$ and parallel $\mathbf{E}_\parallel$ to the c axis. Present results (solid line) are compared to the experimental room-temperature results of Cardona and Harbeke (Ref. 1) (dashed lines). The labels correspond to experimentally observed critical points (Ref. 1).

framework is adequate for this early transition-metal oxide.

The fundamental absorption edge for $\mathbf{E}_\perp$ occurs at 2.02 eV, resulting from transitions between the topmost valence band and the bottom of the conduction band along the Δ and Σ directions. Beyond the absorption edge, experimental reflectivity[1] and electroreflectance[2] measurements reveal two prominent features, designated as A_1 and A_2 in Fig. 2, and have been attributed to splitting in the O $2p_{x,y}$ orbitals.[5] The first major peak, which we attribute to A_1, occurs at 3.06 eV and results from transitions between the top of the valence band to the bottom of the conduction band in the neighborhood of the R-A direction. The next major peak, which we assign to A_2, occurs at 4.67 eV and results from transition between the top four valence bands and the t_{2g} conduction-band states in the neighborhood of Γ. Between these two peaks, we find two additional features which have not been observed experimentally.[1] The first feature appears at 3.6 eV, resulting from transitions between valence bands 14–15 to the first two conduction bands along the Σ direction near Γ. (We label the valence bands from 1–16 and the conduction bands from 1 upwards.) The second feature occurs at 3.94 eV and results from transitions between valence bands 14–15 to the lowest three conduction bands in the neighborhood of the Σ direction. The predicted separation between the A_1 and A_2 peaks was found to be 1.7 eV which is in good agreement with the experimental value of 1.4 eV.[1] Three other structural features, labeled as B_1, B_2, and C in Fig. 2, have been observed experimentally at higher energy. We find similar high-energy structural features; the first occurring at 6.06 eV is attributed to B_1. The majority of the structure occurs for transitions between valence bands 10–12 and the bottom five conduction-band states of t_{2g} symmetry as well as transition from valence band 15 to the first conduction-band state of e_g symmetry. These transitions occur in the neighborhood of the A-Z direction. The next high-energy structure is associated with B_2 and occurs at 6.96 eV resulting from transitions between valence bands 14–16 and the first two conduction bands of e_g symmetry in the neighborhood of Γ. The structure attributed to C occurs at 7.59 eV and results from transitions between valence bands 11–12 and the first two conduction-band states of e_g symmetry in the neighborhood of the T direction. We find an additional feature at 8.11 eV resulting from two critical points. The first, near Γ, results from transitions between valence bands 14–15 to conduction band 10. The second critical point occurs near A and results from transitions between valence bands 10–11 and conduction bands 7–8.

The absorption edge for $\mathbf{E}_\parallel$ polarization occurs at 2.05 eV resulting from transitions between the top of the valence band and the bottom of the conduction band with the majority of the structure occurring along the Δ direction. As seen in Fig. 2, only one prominent feature, labeled A, has been experimentally[1,2] observed for $\mathbf{E}_\parallel$ and has been attributed to transitions from the O $2p_z$ orbitals.[5] Unlike the case of $\mathbf{E}_\perp$ polarization, we find a rather broad absorption edge (peak A) for $\mathbf{E}_\parallel$. This is often the case in comparing theoretical to experimental results as many-body effects, e.g., excitons, can strongly modify the structural features of the absorption edge.[7] Although absorption experiments[5] reveal exciton behavior for the direct-forbidden transition, they are only weakly allowed for $\mathbf{E}_\perp$ and strictly forbidden for $\mathbf{E}_\parallel$ polarization.[5] The first major peak for $\mathbf{E}_\parallel$ polarization occurs at 3.06 eV resulting from two critical points. The first, near Γ, is a result of transitions between valence band 14 to the bottom of the conduction band. The second critical point occurs near R and results from transitions between the top of the valence band to the bottom of the conduction band. The second major peak occurs at 3.9 eV and results from transitions between the top four valence bands and the lowest four conduction bands along the Σ and Y directions near M. Two other features on the high-energy side of this peak appear as shoulders at 4.47 and 4.67 eV, respectively, and result from transitions between valence bands 12–13 to conduction bands 2 and 4 along Δ. The next major feature appears at 6.15 eV resulting from transition between valence bands 11–12 to conduction bands 3–5 with t_{2g} symmetry and valence band 15 to conduction band 7 with e_g symmetry. The transitions are located near the neighborhood of the Z-A-R face and is associated with peak B. The next major peak occurs at 7.27 eV and is a result of transitions between valence bands 12–14 and conduction bands 7–8 located in the neighborhood of the M-Z direction and is associated with peak C. We find an additional peak composed of two critical points at 8.07 and 8.25 eV resulting from transitions between valence bands 14–15 to conduction band 10 near Γ along the Δ and Σ directions and valence bands 10–12 to conduction bands 7–8 in the neighborhood of the Z-R direction.

In summary, we have self-consistently calculated the band structure of TiO_2 within the LDA formalism using *ab initio* pseudopotentials and a plane-wave basis. Our calculations yield good results for the fine structure in the imaginary part of the dielectric function as compared to experimental results. Specifically, we are able to account for differences in the electronic polarizations for the dielectric functions. Our results suggest that for this early-transition-metal oxide, accurate optical matrix elements are described within the LDA.

We would like to acknowledge support for this work by the Division of Materials Research, Office of Basic Energy Sciences, U.S. Department of Energy, under Grant No. DE-FG02-89ER45391 and by the Minnesota Supercomputer Institute.

[1] M. Cardona and G. Harbeke, Phys. Rev. **137**, A1467 (1965).

[2] A. Frova, P. J. Boddy, and Y. S. Chen, Phys. Rev. **157**, 700 (1967).

[3] K. Vos and H. J. Krusemeyer, Solid State Commun. **15**, 949 (1974); J. Phys. C **10**, 3893 (1977).

[4] F. Arntz and Y. Yacoby, Phys. Rev. Lett. **17**, 857 (1966).

[5] J. Pascual, J. Camassel, and H. Mathieu, Phys. Rev. Lett. **39**, 1490 (1977); Phys. Rev. B **18**, 5606 (1978).

[6] H. Mathieu, J. Pascual, and J. Camassel, Phys. Rev. B **18**, 6920 (1978); J. Camassel, J. Pascual, and H. Mathieu, *ibid.* **20**, 5292 (1979).

[7] M. L. Cohen and J. R. Chelikowsky, in *Electronic Structure and Optical Properties of Semiconductors*, 2nd ed., edited by M. Cardona (Springer-Verlag, Berlin, 1989).

[8] P. Hohenberg and W. Kohn, Phys. Rev. **136**, B864 (1964); W. Kohn and L. J. Sham, Phys. Rev. **140**, A1133 (1965).

[9] *Theory of the Inhomogeneous Electron Gas*, edited by S. Lundqvist and N. H. March (Plenum, New York, 1983); W. E. Pickett, Comput. Phys. Rep. **9**, 115 (1989); R. O. Jones and O. Gunnarsson, Rev. Mod. Phys. **61**, 689 (1989), and references therein.

[10] M. S. Hybertsen and S. G. Louie, Phys. Rev. Lett. **55**, 1418 (1985); Phys. Rev. B **34**, 5390 (1986); X. Zhu and S. G. Louie, *ibid.* **43**, 14142 (1991), and references therein.

[11] J. P. Perdew and M. Levy, Phys. Rev. Lett. **51**, 1884 (1983).

[12] A. Svane and O. Gunnarsson, Phys. Rev. Lett. **65**, 1148 (1990).

[13] R. A. Heaton, J. G. Harrison, and C. C. Lin, Phys. Rev. B **28**, 5992 (1983).

[14] K. M. Glassford, N. Troullier, J. L. Martins, and J. R. Chelikowsky, Solid State Commun. **76**, 635 (1990).

[15] J. L. Martins and M. L. Cohen, Phys. Rev. B **37**, 6134 (1988); J. L. Martins, N. Troullier, and S.-H. Wei, *ibid.* **43**, 2213 (1991).

[16] D. M. Ceperley and B. J. Adler, Phys. Rev. Lett. **45**, 566 (1980); J. P. Perdew and A. Zunger, Phys. Rev. B **23**, 5048 (1981).

[17] N. Troullier and J. L. Martins, Solid State Commun. **74**, 613 (1990); Phys. Rev. B **43**, 1993 (1991).

[18] L. Kleinman and D. M. Bylander, Phys. Rev. Lett. **48**, 1425 (1982).

[19] H. Ehrenreich and M. H. Cohen, Phys. Rev. **115**, 786 (1959).

[20] S.-Y. Ren and W. A. Harrison, Phys. Rev. B **23**, 762 (1981).

[21] S. P. Kowalczyk, F. R. McFeely, L. Ley, V. T. Gritsyna, and D. A. Shirley, Solid State Commun. **23**, 161 (1977).

[22] N. I. Medvedeva, V. P. Zhukov, M. Ya. Khodos, and V. A. Gubanov, Phys. Status Solidi (b) **160**, 517 (1990).

[23] V. P. Gupta and N. M. Ravindra, J. Phys. Chem. Solids **41**, 591 (1980).